Direct production of 4-hydroxybenzoic acid from cellulose using cellulase-displaying Pichia pastoris

Inokuma, Kentaro ; Miyamoto, Shunya ; Morinaga, Kohei ; Kobayashi, Yuma ; Kumokita, Ryota ; Bamba, Takahiro ; Ito, Yoichiro ; Kondo, Akihiko ;…

(Citation)
Biotechnology and Bioengineering,120(4):1097-1107

(Issue Date)
2023-04

(Resource Type)
journal article

(Version)
Accepted Manuscript

(URL)
https://hdl.handle.net/20.500.14094/0100479390

Graphical Abstract

A recombinant *Pichia pastoris* strain co-displaying three cellulases and expressing chorismate pyruvate-lyase was constructed for direct production of 4-hydroxybenzoic acid (4-HBA) from cellulose. This strain produced 975 mg/L of 4-HBA from phosphoric acid swollen cellulose, with a yield of 11.6% after 96 h of batch fermentation without commercial cellulase addition.

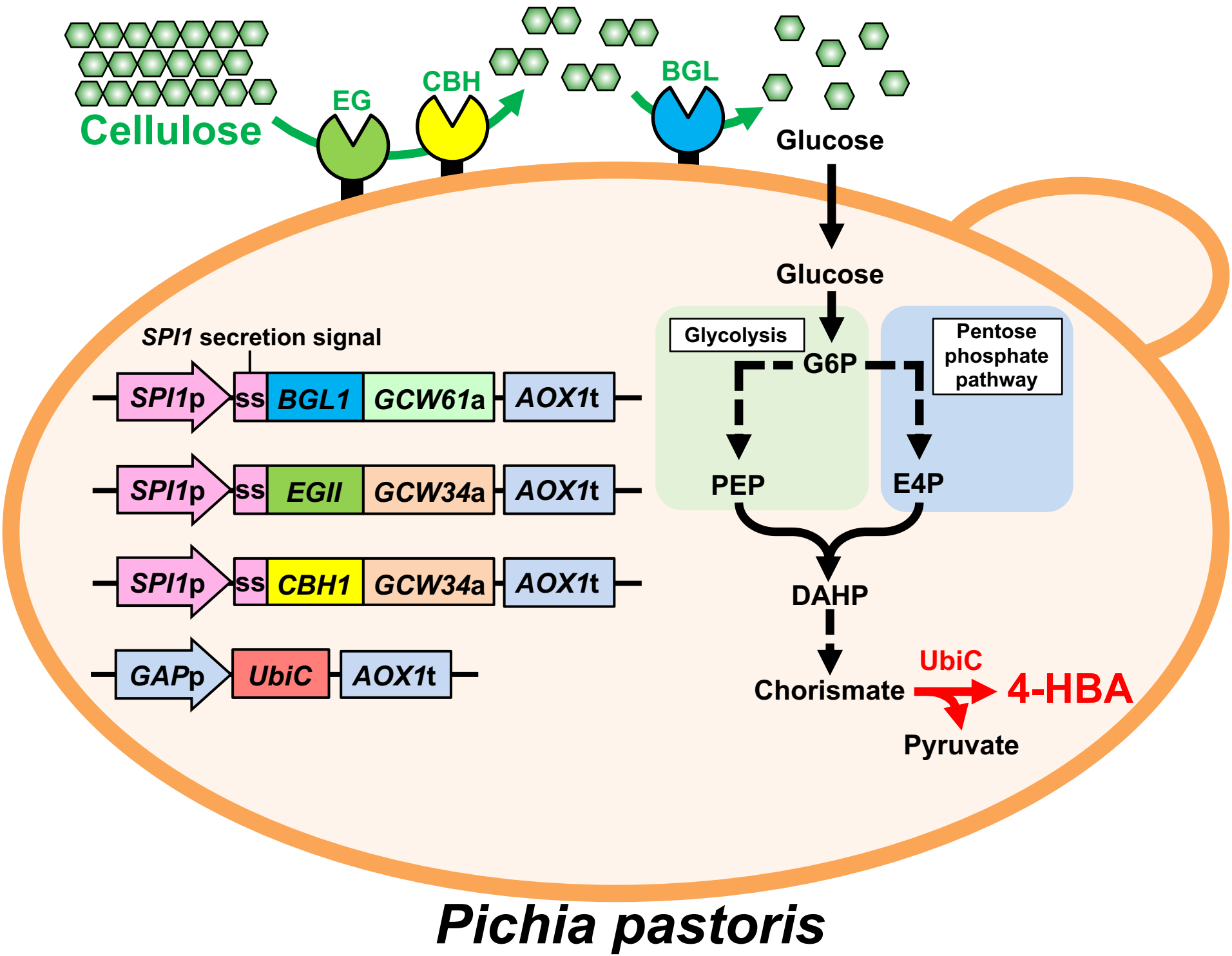
Cellulose
EG
CBH
BGL
Glucose
Glucose
Glycolysis
G6P
Pentose phosphate pathway
PEP
E4P
DAHP
Chorismate
UbiC
4-HBA
Pyruvate
SPI1 secretion signal
SPI1p
ss
BGL1
GCW61a
AOX1t
SPI1p
ss
EGII
GCW34a
AOX1t
SPI1p
ss
CBH1
GCW34a
AOX1t
GAPp
UbiC
AOX1t
Pichia pastoris

Direct production of 4-hydroxybenzoic acid from cellulose using cellulase-displaying *Pichia pastoris*.

Kentaro Inokuma,[1] Shunya Miyamoto,[1] Kohei Morinaga,[1] Yuma Kobayashi,[1] Ryota Kumokita,[1] Takahiro Bamba,[2] Yoichiro Ito[2], Akihiko Kondo,[1,2,3] Tomohisa Hasunuma,[1,2,*]

[1] Graduate School of Science, Technology and Innovation, Kobe University, 1-1 Rokkodai-cho, Nada-ku, Kobe 657-8501, Japan

[2] Engineering Biology Research Center, Kobe University, 1-1 Rokkodai-cho, Nada-ku, Kobe 657-8501, Japan

[3] Biomass Engineering Program, RIKEN, 1-7-22 Suehiro-cho, Tsurumi-ku, Yokohama, Kanagawa 230-0045, Japan

* Corresponding author:
Tomohisa Hasunuma
Telephone: +81-78-803-6461, Fax: +81-78-803-6362
E-mail: hasunuma@port.kobe-u.ac.jp

Running title

Direct 4-HBA production from cellulose

Abstract

4-hydroxybenzoic acid (4-HBA) is an industrially important aromatic compound, and there is an urgent need to establish a bioprocess to produce this compound in a sustainable and environmentally friendly manner from renewable feedstocks such as cellulosic biomass. Here, we developed a bioprocess to directly produce 4-HBA from cellulose using a recombinant *Pichia pastoris* strain that displays heterologous cellulolytic enzymes on its cell surface via the glycosylphosphatidylinositol (GPI)-anchoring system. β-glucosidase (BGL) from *Aspergillus aculeatus*, endoglucanase (EG) from *Trichoderma reesei*, and cellobiohydrolase (CBH) from *Talaromyces emersonii* were co-displayed on the cell surface of *P. pastoris* using an appropriate GPI-anchoring domain for each enzyme. The cell-surface cellulase activity was further enhanced using *P. pastoris SPI1* promoter- and secretion signal sequences. The resulting strains efficiently hydrolyzed phosphoric acid swollen cellulose (PASC) to glucose. Then, we expressed a highly 4-HBA-resistant chorismate pyruvate-lyase (UbiC) from *Providencia rustigianii* in the cellulase-displaying strain. This strain produced 975 mg/L of 4-HBA from PASC, which corresponding to 36.8% of the theoretical maximum yield, after 96 h of batch fermentation without the addition of commercial cellulase. This 4-HBA yield was over two times higher than that obtained from glucose (12.3% of the theoretical maximum yield). To our knowledge, this is the first report on the direct production of an aromatic compound from cellulose using cellulase-displaying yeast.

Keywords: *Pichia pastoris*, yeast surface display, 4-hydroxybenzoic acid, cellulase, simultaneous saccharification and fermentation

1. Introduction

4-hydroxybenzoic acid (4-HBA) is an important aromatic compound used as a raw material for liquid crystal production. 4-HBA and its derivatives such as parabens also have diverse biological properties and are widely used as additives in many pharmaceuticals, cosmetics, food, and beverages (Manuja et al. 2013). Currently, 4-HBA is chemically produced on an industrial scale using the Kolbe-Schmitt reaction from petroleum-derived phenol (Lindsey and Jeskey 1957). This reaction requires high alkalinity, high-temperature, and high-pressure conditions and produces solid waste such as tar residues (Thomas et al. 2002). Therefore, 4-HBA production from renewable feedstocks under ambient temperature and pressure is attracting attention as an alternative sustainable and environmentally friendly method (Yu et al. 2016).

In plants and microorganisms, 4-HBA is biosynthesized via the shikimate pathway which starts with the condensation of phosphoenolpyruvate (PEP) from glycolysis and erythrose-4-phosphate (E4P) from the pentose phosphate pathway (Averesch and Kromer 2018; Tzin and Galili 2010). After a seven-step reaction, PEP and E4P are converted into chorismate, followed by 4-HBA synthesis via chorismate pyruvate-lyase (UbiC) (Figure 1). Several bioprocesses for 4-HBA production via the shikimate pathway using recombinant microorganisms (*Corynebacterium glutamicum, Escherichia coli*, *Klebsiella pneumoniae*, *Pseudomonas putida,* and *Saccharomyces cerevisiae*) have been reported (Barker and Frost 2001; Kitade et al. 2018; Meijnen et al. 2011; Müller et al. 1995; Verhoef et al. 2007; Yin et al. 2020). The highest reported concentration of microbial 4-HBA production was achieved in an aerobic growth-arrested bioprocess using recombinant *C. glutamicum.* By metabolic engineering for enhancing flux to and through the shikimate pathway and expressing a highly 4-HBA-resistant UbiC from *Providencia rustigianii*, 4-HBA titer of the recombinant *C. glutamicum* was 36.6 g/L after 24 h of incubation using a jar fermenter (Kitade et al. 2018). However, these bioprocesses used model renewable feedstocks such as glucose, xylose, and glycerol as substrates for 4-HBA production. Renewable biomass feedstocks

such as cellulose require high dosages of hydrolytic enzymes for digestion and thereby impede the economic feasibility of direct 4-HBA production from these feedstocks. To our knowledge, there is no report on the direct production of 4-HBA from cellulosic materials.

The cell surface expression of heterologous cellulolytic enzymes is a promising approach to construct whole cell catalysts for the direct production of fuels and chemicals from cellulose. In yeast cells, cellulolytic enzymes (cellulases) can be immobilized in their cell wall via a glycosylphosphatidylinositol (GPI)-anchoring domain, and cellulase-displaying yeast strains have been used for ethanol production from cellulosic substrates (Inokuma et al. 2018). *S. cerevisiae* is the most frequently used yeast species for this system due to its high fermentation capacity and well-developed genetic engineering tools (Ko and Lee 2018; Lian et al. 2018). However, the high ethanol fermentation capacity of *S. cerevisiae* makes it difficult to produce aromatic compounds in high yields (Patra et al. 2021). In fact, the only reported aromatic compound production from cellulosic materials by simultaneous saccharification and fermentation (SSF) using *S. cerevisiae* is resveratrol production from the cellulosic fraction of hydrothermally pretreated *Eucalyptus globulus* wood with the addition of commercial cellulase, and the resveratrol yield was 1.2% of the theoretical maximum value (Costa et al. 2021). To the best of our knowledge, production of aromatic compounds from cellulose by SSF using cellulase-displaying yeast has not been reported.

The Crabtree-negative, methylotrophic yeast *Pichia pastoris* (*Komagataella phaffii*) has several attractive characteristics as a host for cell-surface display, including fast cell growth, high cell density culture, and high secretion of heterologous recombinant proteins compared to *S. cerevisiae* (Karbalaei et al. 2020). Moreover, the metabolism of Crabtree-negative yeasts including *P. pastoris* is well balanced in carbon partitioning among the various pathways including the shikimate pathway (Rajkumar and Morrissey 2020). Kumokita et al. (2022) reported the production of various aromatic compounds produced via the shikimate pathway, including resveratrol, naringenin, norcoclaurine, and reticuline, using metabolically engineered *P. pastoris*. Meanwhile, there are few reports of cell-

surface display of heterologous enzymes in *P. pastoris* compared to that of *S. cerevisiae*, and there is insufficient knowledge of *P. pastoris* as a platform for the GPI-anchoring system. For example, the appropriate GPI-anchoring domains for exo- and endo-cellulases significantly differ in *S. cerevisiae* (Inokuma et al. 2020), while such studies have not been conducted in *P. pastoris*.

In this study, we developed a recombinant *P. pastoris* strain that efficiently displays cellulolytic enzymes on its cell surface via the GPI-anchoring system and used it to directly produce 4-HBA from cellulose. First, we confirmed that *P. pastoris* produces 4-HBA by expression of a heterologous UbiC. Then, the appropriate GPI-anchoring domain for each cellulolytic enzyme was screened to maximize enzyme activity on the *P. pastoris* cell surface. We also evaluated the effect of promoter- and secretion signal sequence on cellulase display efficiency. Finally, SSF of phosphoric acid swollen cellulose (PASC) was conducted using a recombinant *P. pastoris* strain displaying cellulases on its cell surface and expressing UbiC as a whole-cell biocatalyst.

2. Materials and Methods

2.1. Microorganisms and media

Characteristics of all yeast strains used in this work are summarize in Table 1. *P. pastoris* CBS7435 was used as a parent strain. *P. pastoris* strains were cultivated in YPD medium [10 g/L yeast extract, 20 g/L Bacto-peptone (Difco Laboratories, Detroit, MI, USA), and 20 g/L glucose] supplemented with 500 μg/mL G418 (FUJIFILM Wako Pure Chemical, Osaka, Japan), 300 μg/mL hygromycin (Nacalai Tesque), 100 μg/mL Zeocin (Nacalai Tesque), and/or 50 μg/mL clonNAT (Jena Bioscience, Löbstedter, Germany) as required. *Escherichia coli* strain DH5α (Toyobo, Osaka, Japan) was used for construction and amplification of plasmid DNA. The medium for *E. coli* growth was prepared as previously described (Inokuma et al. 2016a).

2.2. Plasmid construction and yeast transformation

The plasmids and primers used in this study are listed in Table 1 and Supplementary Table S1, respectively. Detailed methods for construction of plasmids and yeast strains were provided as Supplementary Text S1.

2.3. 4-HBA production from glucose

Yeast cells were pre-cultured at 30 °C in 5 mL of YPD medium supplemented with 500 μg/mL G418 in a BR-43FL shaker incubator (200 rpm; Taitec, Saitama, Japan) for 18 h. This was used to inoculate 20 mL of YPD medium in 100-mL Erlenmeyer flasks at an initial cell density (OD_{600}) of 0.05, and cultivated at 30 °C and 150 rpm in a shaker incubator. The culture broth was sampled every 24 h for 3 days and the glucose concentration in each sample was determined using high-performance liquid chromatography (HPLC) (Shimadzu, Kyoto, Japan) as previously described (Inokuma et al. 2016b). 4-HBA concentration in the culture medium was assessed using HPLC equipped with a Cosmosil $5C_{18}$-AR-II column (4.6 × 250 mm; Nacalai Tesque, Kyoto, Japan) and an SPD-20A UV/VIS detector (Shimadzu). The column was kept at 40 °C, and acetonitrile/H_2O (30:70) containing 0.1% (v/v) formic acid was used as the mobile phase at a flow rate of 1.0 mL/min. 4-HBA was detected by absorbance at 280 nm.

2.4. Preparation of cellulase-displaying yeast cells

P. pastoris strains were pre-cultured in 5 mL of YPD medium supplemented with appropriate antibiotics at 30 °C and 200 rpm for 18 h, inoculated in 50 mL (for enzyme assays) or 400 mL (for cellulolytic activity assay and direct 4-HBA production from cellulose) of YPD medium in Erlenmeyer flasks at an initial OD_{600} of 0.05, and cultivated at 30 °C and 150 rpm for 48 h in a shaker incubator. The cells were collected by centrifugation at 1000×*g* for 5 min and washed twice with distilled water. The washed cell pellets were used in the following experiments.

146 **2.5. Enzyme assays**

147 β-glucosidase (BGL) and endoglucananse (EG) activities of yeast cells were evaluated using *p*-
148 nitrophenyl-*β*-D-glucopyranoside (*p*NPG, Sigma-Aldrich, Saint Louis, MO, USA) using AZCL-HE-
149 cellulose (Cellazyme C tablets; Megazyme, Bray, Ireland) as the substrates, respectively, according
150 to previous methods (Inokuma et al. 2016a).

151

152 **2.6. Cellulolytic activity assay**

153 PASC was prepared from Avicel PH-101 (Sigma-Aldrich) as previously described (Den Haan et
154 al. 2007). The cellulolytic activity of yeast cells was measured using PASC according to a previously
155 described method with slight modifications (Liu et al. 2016). Briefly, the reaction mixture contained
156 1% (w/v) PASC, 50 mM sodium citrate buffer (pH 5.0), 100 mM methyl glyoxal (Nacalai Tesque,
157 Inc., Kyoto, Japan), and 100 g wet cell/L of yeast cell suspension. The reaction was carried out at
158 50 °C for 60 min while rotating at 35 rpm using a heat block (Thermo Block Rotator SN- 06BN;
159 Nissin, Tokyo, Japan) and the glucose concentration in the supernatant was quantified using
160 LabAssay Glucose (FUJIFILM Wako Pure Chemical Corporation, Osaka, Japan). One unit of
161 cellulolytic activity was defined as the activity that released 1 μmol of glucose per min.

162

163 **2.7. Direct 4-HBA production from cellulose**

164 The fermentation medium contained 10 g/L yeast extract, 20 g/L Bacto-peptone (Difco
165 Laboratories, Detroit, MI, USA), 50 mM sodium citrate buffer (pH 5.0), and 10 g/L PASC. Yeast
166 cells were inoculated into 10 mL of the fermentation medium in 100-mL screw-cap bottles at an
167 initial cell concentration of 100 g wet cells/L, and fermentation was conducted at 35 °C with stirring
168 at 150 rpm. The fermentation medium was sampled every 24 h for 4 days and their 4-HBA
169 concentrations were determined as described above.

170

171 **2.8. Tolerance assay**

172 *P. pastoris* CBS7435 was pre-cultivated in 5 mL of YPD medium at 30°C and 200 rpm for 18 h,
173 then inoculated into 5 mL of YPD medium supplemented with various 4-HBA concentrations (0,
174 0.5, 1.0, 3.0, and 5.0 g/L) in L-shaped test tubes at an initial OD_{660} of 0.05. Cell growth was monitored
175 every 30 min using a TVS062CA Bio-photorecorder (Advantec Toyo, Tokyo, Japan) at 30°C and
176 70 rpm.

177

178 **2.9. Statistical analysis**

179 The data are presented as the mean ± standard deviation of three independent experiments.
180 Significant differences between groups of values were calculated according to paired comparisons
181 using Student's *t*-tests using the Excel software (Microsoft-365). Difference with confidence level of
182 95% ($p < 0.05$) was considered statistically significant.

183

184 **3. Results**

185 **3.1. Construction of the recombinant *P. pastoris* strain for 4-HBA production**

186 Wild type *P. pastoris* lacks the enzyme required to convert chorismate to 4-HBA (UbiC).
187 Therefore, heterologous expression of UbiC was conducted in *P. pastoris* to confirm that 4-HBA can
188 be produced by this yeast. A highly 4-HBA-resistant UbiC from the intestinal bacterium *P.*
189 *rustigianii* (PrUbiC) was employed because it achieved the highest reported 4-HBA production in *C.*
190 *glutamicum* (Kitade et al. 2018). The PrUbiC expression cassette was constructed under the control
191 of the endogenous promoter of glyceraldehyde-3-phosphate dehydrogenase (*GAP*) and integrated
192 into the *P. pastoris* CBS7435 genome to construct the Pp-UbiC strain. This strain produced 594 ±
193 54 mg/L of 4-HBA from 20 g/L glucose after 48 h fermentation in YPD medium, while its parent
194 strain (CBS7435) did not show significant 4-HBA production (Figure 2).

195

3.2. Screening of GPI-anchoring domains for cell-surface cellulase display in *P. pastoris*

The hydrolysis of cellulose to glucose requires the cooperative action of multiple hydrolytic enzymes (cellulases) with different roles. It is important to select the appropriate GPI-anchoring domain for each enzyme to maximize cellulase hydrolytic activity on the yeast cell surface (Inokuma et al. 2020). Thirteen cell wall proteins can be used as GPI-anchoring domains for lipase cell-surface display in *P. pastoris* (Zhan et al. 2013), while Sed1p from *S. cerevisiae* is one of the most widely used GPI-anchoring domains for yeast cell surface display of heterologous proteins including lipase display in *P. pastoris* (Su et al. 2010). These 14 GPI-cell wall proteins were fused to the C-terminus of *Aspergillus aculeatus* β-glucosidase 1 (BGL1) and *Trichoderma reesei* endoglucanase II (EGII) to identify the appropriate GPI-anchoring domain for each cellulase. The expression cassettes of these fusion proteins with the *GAP* promoter and the secretion signal from *S. cerevisiae* alpha-factor (Ito. et al. 2022) were integrated into the *P. pastoris* CBS7435 genome, and the cell-surface enzyme activities of the constructed strains were evaluated as described in the Materials and Methods. BGL1 activity was detected from the yeast cell surface in all GPI-anchoring domains tested in this study (Figure 3a). There was a 3- to 4-fold variation in BGL activity depending on the GPI-anchoring domain used; the highest cell-surface activity was observed using GCW61 as the GPI-anchoring domain. These trends are like those previously reported for lipase (Zhang et al. 2013). In contrast, EG activity markedly changed depending on the fused GPI-anchoring domains (Figure 3b); the highest EG activity was observed using GCW34, while GCW61 was unsuitable for EG display. Meanwhile, both BGL- and EG activity was relatively high using GCW30- and GCW51 GPI-anchoring domains.

3.3. Improving cell-surface cellulase activity by replacing promoter- and secretion signal sequences

220 We previously reported that the utilization of promoter and secretion signal sequence of genes
221 encoding GPI-anchoring cell wall proteins improves cellulase display efficiency (Inokuma et al.
222 2016a; Inokuma et al. 2014). *P. pastoris SPI1* encodes a GPI-anchoring cell wall protein
223 corresponding to GCW14 in Figure 3, and its promoter has been used as the strong constitutive
224 promoter comparable to *GAP* promoter in *P. pastoris* (Ata et al. 2017). Therefore, the *GAP* promoter
225 and the secretion signal from *S. cerevisiae* alpha-factor of the expression cassette for BGL and EGII
226 display were replaced by those derived from *P. pastoris SPI1*. The *SPI1* promoter and the *SPI1*
227 secretion signal exhibited approximately 1.3- and 2.4-fold higher cell-surface BGL and EG activity
228 compared with the conventional *GAP* promoter and the secretion signal from *S. cerevisiae* alpha-
229 factor, respectively (Figure 4a and b).
230
231 **3.4. Construction of a *P. pastoris* strain co-displaying BGL, EG, and CBH**
232 Three major types of cellulases (BGL, EG, and CBH) that play important roles in the hydrolysis
233 of cellulose to glucose were co-displayed on the cell surface of *P. pastoris* to produce 4-HBA from
234 cellulose. *A. aculeatus* BGL1 and *T. reesei* EGII were fused with the GPI-anchoring domains that
235 exhibited the highest activity in Figure 3, respectively (BGL1-GCW61 and EGII-GCW34).
236 *Talaromyces emersonii* CBH1 was fused with GCW34 (CBH1-GCW34) to make it work
237 collaboratively with EGII. Gene cassettes for the expression of BGL1-GCW61, EGII-GCW34, and
238 CBH1-GCW34 with the *SPI1* promoter and the *SPI1* secretion signal were integrated into the
239 genome of *P. pastoris* CBS7435 to construct the Pp-BEC strain. Then, the cellulolytic activity of the
240 constructed strain to change cellulose to glucose was evaluated. The cellulolytic reaction was
241 performed at 50°C with the addition of methylglyoxal to completely inhibit glucose uptake in *P.*
242 *pastoris* cells. The Pp-BEC strain produced approximately 1.4 g/L of glucose from PASC within the
243 first 1 h of the reaction, and approximately 4.0 g/L at 18 h (Figure 5). This result clearly indicated
244 that this strain acquired the ability to break down cellulose to glucose by cell-surface display of the

245 cellulases. The gradually declining glucose production rate over time is probably due to product
246 inhibition of the cellulases by glucose accumulation. The PASCase activity of this strain was 8.36 ±
247 0.71 U/g dry cells based on glucose produced within the first 1 h.
248
249 **3.5. Direct 4-HBA production from cellulose**
250 The PrUbiC expression cassette was integrated into the genome of the Pp-BEC strain to achieve
251 direct 4-HBA production from cellulose. Then, SSF of cellulose (PASC) was performed using the
252 Pp-BEC-UbiC strain as a whole-cell biocatalyst. The Pp-UbiC strain expressing only PrUbiC
253 produced 59 ± 6 mg/L 4-HBA after 96 h of fermentation. Since this strain produced similar amounts
254 of 4-HBA in the fermentation without PASC (Supplementary Figure S1), the 4-HBA production was
255 probably derived from carbon sources other than cellulose such as yeast extract, peptone, and citrate
256 used as a buffer. Meanwhile, the Pp-BEC-UbiC strain displaying cellulases and expressing PrUbiC
257 produced 975 ± 22 mg/L of 4-HBA from 10 g/L of PASC (Figure 6). Based on stoichiometric
258 network analysis, theoretical maximum yield of 4-HBA from glucose in yeast under anaerobic
259 condition is 242 mg/g glucose (Krömer et al. 2013). Since complete hydrolysis of 10 g/L cellulose
260 yields 11 g/L of glucose, the 4-HBA titer of the Pp-BEC-UbiC strain corresponds to 36.8% of the
261 theoretical maximum yield.
262
263 **4. Discussion**
264 4-HBA is an industrially important aromatic compound and there is an urgent need to establish a
265 bioprocess to produce it from renewable feedstocks such as cellulosic biomass in a sustainable and
266 environmentally friendly manner. However, there are no reports on the direct production of 4-HBA
267 from cellulose due to the need for high-dosages of costly commercial cellulases for the hydrolysis of
268 cellulose to glucose. In this study, a recombinant *P. pastoris* strain was constructed containing both
269 cellulolytic- and 4-HBA production capacities by displaying three cellulases (BGL, EG, and CBH)

on the yeast cell surface and expressing a highly 4-HBA-resistant chorismate pyruvate-lyase (PrUbiC). The constructed strain (Pp-BEC-UbiC) produced 4-HBA from cellulose substrate (PASC) without the addition of any commercial cellulase (Figure 6). To our knowledge, this is the first report on the direct production of 4-HBA by SSF of cellulose. Moreover, this is the first bioproduction of an aromatic compound by SSF using cellulase-displaying yeast.

Cell-surface display of multiple cellulases in *P. pastoris* was previously reported by Dong et al. (2020); cellulases were produced by recombinant *E. coli* and then immobilized on the cell surface of *P. pastoris* expressing scaffold proteins (Dong et al. 2020). In contrast, this study constructed recombinant *P. pastoris* expressing cellulases by itself and immobilizing them on the cell surface via GPI-anchoring domains, which is a more cost-effective consolidated bioprocess.

The cell-surface cellulase activity was enhanced by screening the GPI-anchoring domains and adopting the promoter and secretion signal derived from *P. pastoris SPI1*. The *P. pastoris* strain expressing *A. aculeatus* BGL1 fused with the GCW61 under the control of the *SPI1* promoter and the *SPI1* secretion signal (Pp-BG-SSG61) showed cell-surface BGL activity of 3399 U/g dry cells. This was approximately 2.7-fold higher than that of the previously recorded highest level in *S. cerevisiae* (1250 U/g dry cells) in our previous study (Inokuma et al. 2021) measured by the same method. Although no reports have directly compared the performance of *S. cerevisiae* and *P. pastoris* as hosts for yeast cell-surface display technology, these results clearly demonstrate the potential of *P. pastoris* as a host for this technology.

T. reesei EGII showed an entirely different suitability of GPI-anchoring domains than that of *A. aculeatus* BGL1. The cell surface EG activity markedly changed depending on the fused GPI-anchoring domains, and the highest EG activity was observed using GCW34 (Figure. 3b). This phenomenon may be because the localization tendency of the target protein in the yeast cell wall differs depending on the GPI-anchoring domains. Our previous study with *S. cerevisiae* suggested that the GPI-anchoring domain affects not only the cell-surface display efficiency of target proteins,

295 but also their anchorage position in the cell wall (Inokuma et al. 2020). The anchorage position of the
296 enzyme, and the depth in the cell wall is a particularly important factor for yeast cell-surface display
297 because the yeast cell wall is a thick structure composed of microfibrillar array of glucan chains
298 (Dupres et al. 2010). Cellobiose and *p*NPG are small molecule substrates with relatively easy access
299 to the BGL binding site. Meanwhile, macromolecules such as the water-insoluble cellulose substrate
300 can only access EG that are exposed on the external surface of the cell wall. GCW34 may be a
301 promising GPI-anchoring domain to display the enzyme to the external surface of the *P. pastoris* cell
302 wall. However, further investigations such as immunoelectron-microscopic observation are required.
303 GCW30 and GCW51 exhibit relatively high activity in both BGL and EG; therefore they are
304 potential options as versatile GPI-anchoring domains in *P. pastoris*.
305 The 4-HBA yield from PASC by the Pp-BEC-UbiC strain was 36.8% of the theoretical maximum
306 yield based on stoichiometric network analysis. This was over two times higher than that obtained
307 from glucose by the Pp-UbiC strain (12.3% of the theoretical maximum yield). This is probably due
308 to the slow glucose release in PASC fermentation. Significant improvements in the yields of aromatic
309 compounds produced via the shikimate pathway by glucose limitation were previously reported in *S.*
310 *cerevisiae* (Liu et al. 2021; Liu et al. 2019) and *Scheffersomyces stipitis* yeasts (Kobayashi et al. 2021).
311 This is likely due to the higher flux from the pentose phosphate pathway under glucose-limited
312 conditions resulting in higher E4P availability compared to normal batch conditions (Liu et al. 2019).
313 SSF of cellulose which slowly releases glucose might be a promising approach for producing
314 aromatic compounds in high yields.
315 Nevertheless, the titer (975 mg/L) and yield (36.8%) of 4-HBA from PASC by the Pp-BEC-UbiC
316 strain is too low to apply the bioproduction process on a commercial basis. Thus, it is essential to
317 improve the 4-HBA titer and yield of recombinant *P. pastoris*. The highest reported titer of microbial
318 4-HBA production using metabolically engineered *C. glutamicum* expressing PrUbiC is 36.6 g/L
319 after 24 h incubation in fed-batch fermentation by overexpressing genes in the shikimate pathway

and deleting genes involved in by-product formation (Kitade et al. 2018). Employing similar metabolic engineering strategies may be effective in improving 4-HBA productivity in *P. pastoris*.

Phenolic acids including 4-HBA can be toxic compounds for microorganisms (Valanciene et al. 2020) and this must be overcome for the commercialization of 4-HBA production using a recombinant *P. pastoris* strain. The cell growth of *P. pastoris* CBS7435 was inhibited by 4-HBA > 1 g/L, and this strain did not grow at 5 g/L of 4-HBA (Supplementary Figure S2). This concentration is lower than that of *E. coli* and *C. glutamicum* (Barker and Frost 2001; Kitade et al. 2018) which have been reported to achieve over 10 g/L of 4-HBA production. This indicates that *P. pastoris* is more sensitive to 4-HBA than these bacteria. Therefore, it is necessary to improve 4-HBA tolerance of *P. pastoris* by genetic engineering or to develop a technology to remove this compound from the fermentation system to achieve over 5 g/L of 4-HBA production using a recombinant *P. pastoris* strain. This may be possible using *in situ* two-phase extractive fermentation systems combining organic solvents as extractants with the fermentation medium to overcome the microbial toxicity of phenolic compounds (Luo et al. 2019; Salgado et al. 2014).

5. Conclusions

Direct production of 4-HBA was demonstrated through SSF of cellulose using a recombinant *P. pastoris* strain co-displaying three cellulases (BGL, EG, and CBH) and expressing PrUbiC. The recombinant *P. pastoris* strain produced 975 mg/L of 4-HBA from PASC, with a yield of 36.8% after 96 h of batch fermentation without commercial cellulase addition. These results indicate that SSF using cellulase-displaying yeast is a sustainable and environmentally friendly technology to produce 4-HBA as an alternative to its chemical synthesis, and that *P. pastoris* has high potential for this bioprocess. However, metabolic engineering of recombinant *P. pastoris* is required to improve the 4-HBA titer and yield. Furthermore, countermeasures are required against the microbial toxicity of 4-HBA to apply this bioprocess on a commercial basis.

Data availability statement

All data generated or analyzed during this study were included in this published article.

Acknowledgements

We thank Misa Ishigami for technical assistance. We are also grateful for support from NEDO Project P20011 (Development of bioderived product production technology that accelerates the realization of carbon recycling).

Conflict of Interest Statement

The authors declare that they have no competing interests.

Ethical approval Statement

This article does not contain any studies with human participants or animals performed by any of the authors.

Author Contribution Statement

Kentaro Inokuma, Shunya Miyamoto, Kohei Morinaga, and Yoichiro Ito conducted experiments. Kentaro Inokuma, Yuma Kobayashi, Ryota Kumokita, and Takahiro Bamba conceived the topic and designed the study. Kentaro Inokuma analyzed the results and wrote the manuscript with support from Tomohisa Hasunuma. Akihiko Kondo and Tomohisa Hasunuma supervised all aspects of the study. All authors read and approved the manuscript.

References

Ata, Ö., Prielhofer R, Gasser, B., Mattanovich, D., & Çalık, P. (2017). Transcriptional engineering of the glyceraldehyde-3-phosphate dehydrogenase promoter for improved heterologous protein production in *Pichia pastoris*. *Biotechnology and Bioengineering*, *114*(10), 2319-2327. *doi:*10.1002/bit.26363

Averesch, N. J. H., & Krömer, J. O. (2018). Metabolic Engineering of the Shikimate Pathway for Production of Aromatics and Derived Compounds-Present and Future Strain Construction Strategies. *Frontiers in Bioengineering and Biotechnology*, *6*, 32. *doi:*10.3389/fbioe.2018.00032

Barker, J. L., & Frost, J. W. (2001). Microbial synthesis of *p*-hydroxybenzoic acid from glucose. *Biotechnology and Bioengineering*, *76*(4), 376-390. *doi:*10.1002/bit.10160

Costa, C. E., Møller-Hansen, I., Romaní, A., Teixeira, J. A., Borodina, I., & Domingues, L. (2021). Resveratrol Production from Hydrothermally Pretreated Eucalyptus Wood Using Recombinant Industrial *Saccharomyces cerevisiae* Strains. *ACS Synthetic Biology*, *10*(8), 1895-1903. *doi:*10.1021/acssynbio.1c00120

Den Haan, R., Rose, S. H., Lynd, L. R., & van Zyl, W. H. (2007). Hydrolysis and fermentation of amorphous cellulose by recombinant *Saccharomyces cerevisiae*. *Metabolic Engineering*, *9*(1):87-94. *doi:*10.1016/j.ymben.2006.08.005

Dong, C., Qiao, J., Wang, X., Sun, W., Chen, L., Li, S., Wu, K., Ma, L., & Liu, Y. (2020). Engineering *Pichia pastoris* with surface-display minicellulosomes for carboxymethyl cellulose hydrolysis and ethanol production. *Biotechnology for Biofuels*, *13*, 108. *doi:*10.1186/s13068-020-01749-1

Dupres, V., Dufrêne, Y. F., & Heinisch J. J. (2010). Measuring cell wall thickness in living yeast cells using single molecular rulers. *ACS Nano*, *4*(9), 5498-5504. *doi:*10.1021/nn101598v

Inokuma, K., Bamba, T., Ishii, J., Ito, Y., Hasunuma, T., & Kondo, A. (2016a). Enhanced cell-surface display and secretory production of cellulolytic enzymes with *Saccharomyces cerevisiae*

394 Sed1 signal peptide. *Biotechnology and Bioengineering*, *113*(11), 2358-2366.
395 *doi:*10.1002/bit.26008
396 Inokuma, K., Hasunuma, T., & Kondo, A. (2014). Efficient yeast cell-surface display of exo- and
397 endo-cellulase using the *SED1* anchoring region and its original promoter. *Biotechnology for*
398 *Biofuels*, *7*, 8. *doi:*10.1186/1754-6834-7-8
399 Inokuma, K., Hasunuma, T., & Kondo, A. (2016b). Ethanol production from *N*-acetyl-D-
400 glucosamine by *Scheffersomyces stipitis* strains. *AMB Express*, *6*(1), 83.
401 *doi:*10.1186/s13568-016-0267-z
402 Inokuma, K., Hasunuma, T., & Kondo, A. (2018). Whole cell biocatalysts using enzymes displayed
403 on yeast cell surface. In: Chang H (ed.) *Emerging Areas in Bioengineering*, Wiley-VCH,
404 New York, pp 81–92
405 Inokuma, K., Kitada, Y., Bamba, T., Kobayashi, Y., Yukawa, T., den Haan, R., van Zyl, W. H.,
406 Kondo, A., & Hasunuma, T. (2021). Improving the functionality of surface-engineered yeast
407 cells by altering the cell wall morphology of the host strain. *Applied Microbiology and*
408 *Biotechnology*, *105*(14-15), 5895-5904. *doi:*10.1007/s00253-021-11440-6
409 Inokuma, K., Kurono, H., den Haan, R., van Zyl, W. H., Hasunuma, T., & Kondo, A. (2020). Novel
410 strategy for anchorage position control of GPI-attached proteins in the yeast cell wall using
411 different GPI-anchoring domains. *Metabolic Engineering*, *57*, 110-117.
412 *doi:*10.1016/j.ymben.2019.11.004
413 Ito, Y., Ishigami, M., Hashiba, N., Nakamura, Y., Terai, G., Hasunuma, T., Ishii, J., & Kondo, A.
414 (2022). Avoiding entry into intracellular protein degradation pathways by signal mutations
415 increases protein secretion in *Pichia pastoris*. *Microbial Biotechnology*, *15*(9), 2364-2378.
416 *doi:*10.1111/1751-7915.14061
417 Ito, Y., Terai, G., Ishigami, M., Hashiba, N., Nakamura, Y., Bamba, T., Kumokita, R., Hasunuma,
418 T., Asai, K., Ishii, J., & Kondo, A. (2020). Exchange of endogenous and heterogeneous yeast

terminators in *Pichia pastoris* to tune mRNA stability and gene expression. *Nucleic Acids Research*, *48*(22), 13000-13012. *doi:*10.1093/nar/gkaa1066

Karbalaei, M., Rezaee, S. A., & Farsiani, H. (2020). *Pichia pastoris*: A highly successful expression system for optimal synthesis of heterologous proteins. *Journal of Cellular Physiology*, *235*(9), 5867-5881. *doi:*10.1002/jcp.29583

Kitade, Y., Hashimoto, R., Suda, M., Hiraga, K., & Inui, M. (2018). Production of 4-Hydroxybenzoic Acid by an Aerobic Growth-Arrested Bioprocess Using Metabolically Engineered *Corynebacterium glutamicum*. *Applied and Environmental Microbiology*, *84*(6), e02587-17. *doi:*10.1128/AEM.02587-17

Ko, J. K., & Lee, S. M. (2018). Advances in cellulosic conversion to fuels: engineering yeasts for cellulosic bioethanol and biodiesel production. *Current Opinion in Biotechnology*, *50*, 72-80. *doi:*10.1016/j.copbio.2017.11.007

Kobayashi, Y., Inokuma, K., Matsuda, M., Kondo, A., & Hasunuma, T. (2021). Resveratrol production from several types of saccharide sources by a recombinant *Scheffersomyces stipitis* strain. *Metabolic Engineering Communications*, *13*, e00188. *doi:*10.1016/j.mec.2021.e00188

Krömer, J. O., Nunez-Bernal, D., Averesch, N. J. H., Hampe, J., Varela, J., & Varela, C. (2013). Production of aromatics in *Saccharomyces cerevisiae*—A feasibility study. *Journal of Biotechnology*, *163*(2), 184-193. *doi:*10.1016/j.jbiotec.2012.04.014

Kumokita, R., Bamba, T., Inokuma, K., Yoshida, T., Ito, Y., Kondo, A., & Hasunuma, T. (2022). Construction of an L-Tyrosine Chassis in *Pichia pastoris* Enhances Aromatic Secondary Metabolite Production from Glycerol. *ACS Synthetic Biology*, *11*(6), 2098-2107. *doi:*10.1021/acssynbio.2c00047

Lian, J., Mishra, S., & Zhao, H. (2018). Recent advances in metabolic engineering of *Saccharomyces cerevisiae*: New tools and their applications. *Metabolic Engineering*, *50*, 85-108. *doi:*10.1016/j.ymben.2018.04.011

Lindsey, A. S., & Jeskey, H. (1957). The Kolbe-Schmitt Reaction. *Chemical Reviews*, *57*(4), 583-620. *doi:*10.1021/cr50016a001

Liu, Q., Liu, Y., Li, G., Savolainen, O., Chen, Y., & Nielsen, J. (2021). De novo biosynthesis of bioactive isoflavonoids by engineered yeast cell factories. *Nature Communications*, *12*(1), 6085. *doi:*10.1038/s41467-021-26361-1

Liu, Q., Yu, T., Li, X., Chen, Y., Campbell, K., Nielsen, J., & Chen, Y. (2019). Rewiring carbon metabolism in yeast for high level production of aromatic chemicals. *Nature Communications*, *10*(1), 4976. *doi:*10.1038/s41467-019-12961-5

Liu, Z., Ho, S. H., Sasaki, K., den Haan, R., Inokuma, K., Ogino, C., van Zyl, W. H., Hasunuma, T., & Kondo, A. (2016). Engineering of a novel cellulose-adherent cellulolytic *Saccharomyces cerevisiae* for cellulosic biofuel production. *Scientific Reports*, *6*, 24550. *doi:*10.1038/srep24550

Luo, Z. W., Cho, J. S., & Lee, S. Y. (2019). Microbial production of methyl anthranilate, a grape flavor compound. *PNAS*, *116*(22), 10749-10756. *doi:*10.1073/pnas.1903875116

Manuja, R., Sachdeva, A., Jain, A., & Chaudhary, J. (2013). A comparative review on biological activities of *p*-hydroxy benzoic acid and its derivatives. *International Journal of Pharmaceutical Sciences Review and Research*, *22*(2), 109-115.

Meijnen, J. P., Verhoef, S., Briedjlal, A. A., de Winde, J. H., & Ruijssenaars, H. J. (2011). Improved *p*-hydroxybenzoate production by engineered *Pseudomonas putida* S12 by using a mixed-substrate feeding strategy. *Applied Microbiology and Biotechnology*, *90*(3), 885-893. *doi:*10.1007/s00253-011-3089-6

Müller, R., Wagener, A., Schmidt, K., & Leistner, E. (1995). Microbial production of specifically ring-^{13}C-labelled 4-hydroxybenzoic acid. *Applied Microbiology and Biotechnology*, *43*(6), 985-988. *doi:*10.1007/BF00166913

Patra, P., Das, M., Kundu, P., & Ghosh, A. (2021). Recent advances in systems and synthetic biology approaches for developing novel cell-factories in non-conventional yeasts. *Biotechnology Advances*, *47*, 107695. *doi:*10.1016/j.biotechadv.2021.107695

Rajkumar, A. S., & Morrissey, J. P. (2020). Rational engineering of *Kluyveromyces marxianus* to create a chassis for the production of aromatic products. *Microbial Cell Factories*, *19*(1), 207. *doi:*10.1186/s12934-020-01461-7

Salgado, J. M., Rodríguez-Solana, R., Curiel, J. A., de Las, Rivas, B., Muñoz, R., & Domínguez, J. M. (2014). Bioproduction of 4-vinylphenol from corn cob alkaline hydrolyzate in two-phase extractive fermentation using free or immobilized recombinant *E. coli* expressing pad gene. *Enzyme and Microbial Technology*, *58-59*, 22-28. *doi:*10.1016/j.enzmictec.2014.02.005

Su, G. D., Zhang, X., & Lin, Y. (2010). Surface display of active lipase in *Pichia pastoris* using Sed1 as an anchor protein. *Biotechnology Letters*, *32*(8), 1131-1136. *doi:*10.1007/s10529-010-0270-4

Thomas, S. M., DiCosimo, R., & Nagarajan, V. (2002). Biocatalysis: applications and potentials for the chemical industry. *Trends in Biotechnology*, *20*(6), 238-242. *doi:*10.1016/s0167-7799(02)01935-2

Tzin, V., & Galili, G. (2010). New Insights into the Shikimate and Aromatic Amino Acids Biosynthesis Pathways in Plants. *Molecular Plant*, *3*(6), 956-972. *doi:*10.1093/mp/ssq048

Valanciene, E., Jonuskiene, I., Syrpas, M., Augustiniene, E., Matulis, P., Simonavicius, A., & Malys, N. (2020). Advances and Prospects of Phenolic Acids Production, Biorefinery and Analysis. *Biomolecules*, *10*(6), 874. *doi:*10.3390/biom10060874

Verhoef, S., Ruijssenaars, H. J., de Bont, J. A., & Wery, J. (2007). Bioproduction of *p*-hydroxybenzoate from renewable feedstock by solvent-tolerant *Pseudomonas putida* S12. *Journal of Biotechnology*, *132*(1), 49-56. *doi:*10.1016/j.jbiotec.2007.08.031

Yin, H., Hu, T., Zhuang, Y., & Liu, T. (2020). Metabolic engineering of *Saccharomyces cerevisiae* for high-level production of gastrodin from glucose. *Microbial Cell Factories*, *19*(1), 218. *doi:*10.1186/s12934-020-01476-0

Yu, S., Plan, M. R., Winter, G., & Krömer, J. O. (2016). Metabolic Engineering of *Pseudomonas putida* KT2440 for the Production of *para*-Hydroxy Benzoic Acid. *Frontiers in Bioengineering and Biotechnology*, *4*, 90. *doi:*10.3389/fbioe.2016.00090

Zhang, L., Liang, S., Zhou, X., Jin, Z., Jiang, F., Han, S., Zheng, S., & Lin, Y. (2013). Screening for glycosylphosphatidylinositol-modified cell wall proteins in *Pichia pastoris* and their recombinant expression on the cell surface. *Applied and Environmental Microbiology*, *79*(18), 5519-5526. *doi:*10.1128/AEM.00824-13

505 **Table 1** Characteristics of yeast strains and plasmids used in this study

Yeast strains and plasmids	Relevant genotype	Source
P. pastoris		
CBS7435	Wild type	ATCC
Pp-UbiC	CBS7435/pIPrUbiC [GAP_P–*PrUbiC*–$AOX1_T$, $G418^R$]	This study
Pp-BG-GMSed1	CBS7435/pIBG-PpGMSed1 [GAP_P–*MFα*(L42S)$_{SP}$–*A. aculeatus BGL1*–$SED1_A$ -$AOX1_T$, $G418^R$]	This study
Pp-BG-GMG5	CBS7435/pIBG-PpGMG5 [GAP_P–*MFα*(L42S)$_{SP}$–*A. aculeatus BGL1*–$GCW5_A$ -$AOX1_T$, $G418^R$]	This study
Pp-BG-GMG12	CBS7435/pIBG-PpGMG12 [GAP_P–*MFα*(L42S)$_{SP}$–*A. aculeatus BGL1*–$GCW12_A$ -$AOX1_T$, $G418^R$]	This study
Pp-BG-GMG14	CBS7435/pIBG-PpGMG14 [GAP_P–*MFα*(L42S)$_{SP}$–*A. aculeatus BGL1*–$GCW14_A$ -$AOX1_T$, $G418^R$]	This study
Pp-BG-GMG19	CBS7435/pIBG-PpGMG19 [GAP_P–*MFα*(L42S)$_{SP}$–*A. aculeatus BGL1*–$GCW19_A$ -$AOX1_T$, $G418^R$]	This study
Pp-BG-GMG21	CBS7435/pIBG-PpGMG21 [GAP_P–*MFα*(L42S)$_{SP}$–*A. aculeatus BGL1*–$GCW21_A$ -$AOX1_T$, $G418^R$]	This study
Pp-BG-GMG28	CBS7435/pIBG-PpGMG28 [GAP_P–*MFα*(L42S)$_{SP}$–*A. aculeatus BGL1*–$GCW28_A$ -$AOX1_T$, $G418^R$]	This study
Pp-BG-GMG30	CBS7435/pIBG-PpGMG30 [GAP_P–*MFα*(L42S)$_{SP}$–*A. aculeatus BGL1*–$GCW30_A$ -$AOX1_T$, $G418^R$]	This study
Pp-BG-GMG34	CBS7435/pIBG-PpGMG34 [GAP_P–*MFα*(L42S)$_{SP}$–*A. aculeatus BGL1*–$GCW34_A$ -$AOX1_T$, $G418^R$]	This study
Pp-BG-GMG42	CBS7435/pIBG-PpGMG42 [GAP_P–*MFα*(L42S)$_{SP}$–*A. aculeatus BGL1*–$GCW42_A$ -$AOX1_T$, $G418^R$]	This study
Pp-BG-GMG45	CBS7435/pIBG-PpGMG45 [GAP_P–*MFα*(L42S)$_{SP}$–*A. aculeatus BGL1*–$GCW45_A$ -$AOX1_T$, $G418^R$]	This study
Pp-BG-GMG49	CBS7435/pIBG-PpGMG49 [GAP_P–*MFα*(L42S)$_{SP}$–*A. aculeatus BGL1*–$GCW49_A$ -$AOX1_T$, $G418^R$]	This study
Pp-BG-GMG51	CBS7435/pIBG-PpGMG51 [GAP_P–*MFα*(L42S)$_{SP}$–*A. aculeatus BGL1*–$GCW51_A$ -$AOX1_T$, $G418^R$]	This study
Pp-BG-GMG61	CBS7435/pIBG-PpGMG61 [GAP_P–*MFα*(L42S)$_{SP}$–*A. aculeatus BGL1*–$GCW61_A$ -$AOX1_T$, $G418^R$]	This study
Pp-BG-SSG61	CBS7435/pIBG-PpSSG61 [$SPI1_P$–$SPI1_{SP}$–*A. aculeatus BGL1*–$GCW61_A$ -$AOX1_T$, $G418^R$]	This study
Pp-EG-GMSed1	CBS7435/pIBG-PpGMSed1 [GAP_P–*MFα*(L42S)$_{SP}$–*T. reesei EGII*–$SED1_A$ -$AOX1_T$, $G418^R$]	This study

Pp-EG-GMG5	CBS7435/pIBG-PpGMG5 [*GAP*$_P$–*MFα*(L42S)$_{SP}$–*T. reesei EGII–GCW5*$_A$ -*AOX1*$_T$, *G418*^{R}]	This study
Pp-EG-GMG12	CBS7435/pIBG-PpGMG12 [*GAP*$_P$–*MFα*(L42S)$_{SP}$–*T. reesei EGII–GCW12*$_A$ -*AOX1*$_T$, *G418*^{R}]	This study
Pp-EG-GMG14	CBS7435/pIBG-PpGMG14 [*GAP*$_P$–*MFα*(L42S)$_{SP}$–*T. reesei EGII–GCW14*$_A$ -*AOX1*$_T$, *G418*^{R}]	This study
Pp-EG-GMG19	CBS7435/pIBG-PpGMG19 [*GAP*$_P$–*MFα*(L42S)$_{SP}$–*T. reesei EGII–GCW19*$_A$ -*AOX1*$_T$, *G418*^{R}]	This study
Pp-EG-GMG21	CBS7435/pIBG-PpGMG21 [*GAP*$_P$–*MFα*(L42S)$_{SP}$–*T. reesei EGII–GCW21*$_A$ -*AOX1*$_T$, *G418*^{R}]	This study
Pp-EG-GMG28	CBS7435/pIBG-PpGMG28 [*GAP*$_P$–*MFα*(L42S)$_{SP}$–*T. reesei EGII–GCW28*$_A$ -*AOX1*$_T$, *G418*^{R}]	This study
Pp-EG-GMG30	CBS7435/pIBG-PpGMG30 [*GAP*$_P$–*MFα*(L42S)$_{SP}$–*T. reesei EGII–GCW30*$_A$ -*AOX1*$_T$, *G418*^{R}]	This study
Pp-EG-GMG34	CBS7435/pIBG-PpGMG34 [*GAP*$_P$–*MFα*(L42S)$_{SP}$–*T. reesei EGII–GCW34*$_A$ -*AOX1*$_T$, *G418*^{R}]	This study
Pp-EG-GMG42	CBS7435/pIBG-PpGMG42 [*GAP*$_P$–*MFα*(L42S)$_{SP}$–*T. reesei EGII–GCW42*$_A$ -*AOX1*$_T$, *G418*^{R}]	This study
Pp-EG-GMG45	CBS7435/pIBG-PpGMG45 [*GAP*$_P$–*MFα*(L42S)$_{SP}$–*T. reesei EGII–GCW45*$_A$ -*AOX1*$_T$, *G418*^{R}]	This study
Pp-EG-GMG49	CBS7435/pIBG-PpGMG49 [*GAP*$_P$–*MFα*(L42S)$_{SP}$–*T. reesei EGII–GCW49*$_A$ -*AOX1*$_T$, *G418*^{R}]	This study
Pp-EG-GMG51	CBS7435/pIBG-PpGMG51 [*GAP*$_P$–*MFα*(L42S)$_{SP}$–*T. reesei EGII–GCW51*$_A$ -*AOX1*$_T$, *G418*^{R}]	This study
Pp-EG-GMG61	CBS7435/pIBG-PpGMG61 [*GAP*$_P$–*MFα*(L42S)$_{SP}$–*T. reesei EGII–GCW61*$_A$ -*AOX1*$_T$, *G418*^{R}]	This study
Pp-EG-SSG34	CBS7435/pIBG-PpSSG34 [*SPI1*$_P$–*SPI1*$_{SP}$–*T. reesei EGII–GCW34*$_A$ -*AOX1*$_T$, *G418*^{R}]	This study
Pp-BEC	CBS7435/ pIBG-PpSSG61 [*SPI1*$_P$–*SPI1*$_{SP}$–*A. aculeatus BGL1–GCW61*$_A$ -*AOX1*$_T$, *G418*^{R}], pIH-EG-PpSSG34 [*SPI1*$_P$–*SPI1*$_{SP}$–*T. reesei EGII–GCW34*$_A$ -*AOX1*$_T$, *Hyg*^{R}], pIZ-CBH-PpSSG34 [*SPI1*$_P$–*SPI1*$_{SP}$–*T. emersonii CBH1–GCW34*$_A$ -*AOX1*$_T$, *Zeo*^{R}]	This study
Pp-BEC-UbiC	CBS7435/ pIBG-PpSSG61 [*SPI1*$_P$–*SPI1*$_{SP}$–*A. aculeatus BGL1–GCW61*$_A$ -*AOX1*$_T$, *G418*^{R}], pIH-EG-PpSSG34 [*SPI1*$_P$–*SPI1*$_{SP}$–*T. reesei EGII–GCW34*$_A$ -*AOX1*$_T$, *Hyg*^{R}], pIZ-CBH-PpSSG34 [*SPI1*$_P$–*SPI1*$_{SP}$–*T. emersonii CBH1–GCW34*$_A$ -*AOX1*$_T$, *Zeo*^{R}], pIN-PrUbiC [*GAP*$_P$–*PrUbiC–AOX1*$_T$, *NAT*^{R}]	This study
Plasmids		
pPGP_L42S_scFv	*G418*^{R} *GAP*$_P$–*MFα*(L42S)$_{SP}$-*scFv–AOX1*$_T$	(Ito et al. 2022)

pPGPH_DOD	*Hyg*^{R} *GAP*$_{P}$–*MjDOD–AOX1*$_{T}$	(Ito et al. 2020)
pPGPZ-EGFP	*Zeo*^{R} *GAP*$_{P}$–*EGFP–AOX1*$_{T}$	(Kumokita et al. 2022)
pPNS-NHCH	*NAT*^{R} *GAP*$_{P}$–*EcNMCH–AOX1*$_{T}$	(Kumokita et al. 2022)
pIPrUbiC	*G418*^{R} *GAP*$_{P}$–*PrUbiC–AOX1*$_{T}$	This study
pIN-PrUbiC	*NAT*^{R} *GAP*$_{P}$–*PrUbiC–AOX1*$_{T}$	This study
pIBG-SS	*HIS3 SED1*$_{P}$–*GLUA*$_{SP}$–*A. aculeatus BGL1*–*SED1*$_{A}$–*SAG1*$_{T}$	(Inokuma et al. 2014)
pIBG-PpGMSed1	*G418*^{R} *GAP*$_{P}$–*MFα*(L42S)$_{SP}$–*A. aculeatus BGL1*–*SED1*$_{A}$ -*AOX1*$_{T}$	This study
pIBG-PpGMG5	*G418*^{R} *GAP*$_{P}$–*MFα*(L42S)$_{SP}$–*A. aculeatus BGL1–GCW5*$_{A}$ -*AOX1*$_{T}$	This study
pIBG-PpGMG12	*G418*^{R} *GAP*$_{P}$–*MFα*(L42S)$_{SP}$–*A. aculeatus BGL1–GCW12*$_{A}$ -*AOX1*$_{T}$	This study
pIBG-PpGMG14	*G418*^{R} *GAP*$_{P}$–*MFα*(L42S)$_{SP}$–*A. aculeatus BGL1–GCW14*$_{A}$ -*AOX1*$_{T}$	This study
pIBG-PpGMG19	*G418*^{R} *GAP*$_{P}$–*MFα*(L42S)$_{SP}$–*A. aculeatus BGL1–GCW19*$_{A}$ -*AOX1*$_{T}$	This study
pIBG-PpGMG21	*G418*^{R} *GAP*$_{P}$–*MFα*(L42S)$_{SP}$–*A. aculeatus BGL1–GCW21*$_{A}$ -*AOX1*$_{T}$	This study
pIBG-PpGMG28	*G418*^{R} *GAP*$_{P}$–*MFα*(L42S)$_{SP}$–*A. aculeatus BGL1I–GCW28*$_{A}$ -*AOX1*$_{T}$	This study
pIBG-PpGMG30	*G418*^{R} *GAP*$_{P}$–*MFα*(L42S)$_{SP}$–*A. aculeatus BGL1–GCW30*$_{A}$ -*AOX1*$_{T}$	This study
pIBG-PpGMG34	*G418*^{R} *GAP*$_{P}$–*MFα*(L42S)$_{SP}$–*A. aculeatus BGL1–GCW34*$_{A}$ -*AOX1*$_{T}$	This study
pIBG-PpGMG42	*G418*^{R} *GAP*$_{P}$–*MFα*(L42S)$_{SP}$–*A. aculeatus BGL1–GCW42*$_{A}$ -*AOX1*$_{T}$	This study
pIBG-PpGMG45	*G418*^{R} *GAP*$_{P}$–*MFα*(L42S)$_{SP}$–*A. aculeatus BGL1–GCW45*$_{A}$ -*AOX1*$_{T}$	This study
pIBG-PpGMG49	*G418*^{R} *GAP*$_{P}$–*MFα*(L42S)$_{SP}$–*A. aculeatus BGL1–GCW49*$_{A}$ -*AOX1*$_{T}$	This study
pIBG-PpGMG51	*G418*^{R} *GAP*$_{P}$–*MFα*(L42S)$_{SP}$–*A. aculeatus BGL1–GCW51*$_{A}$ -*AOX1*$_{T}$	This study
pIBG-PpGMG61	*G418*^{R} *GAP*$_{P}$–*MFα*(L42S)$_{SP}$–*A. aculeatus BGL1–GCW61*$_{A}$ -*AOX1*$_{T}$	This study
pIBG-PpSSG61	*G418*^{R} *SPI1*$_{P}$–*SPI1*$_{SP}$–*A. aculeatus BGL1–GCW61*$_{A}$ -*AOX1*$_{T}$	This study

pIEG-SS	*HIS3 SED1*$_{P}$–*GLUA*$_{SP}$–*T. reesei EGII–SED1*$_{A}$–*SAG1*$_{T}$	(Inokuma et al. 2014)
pIEG-PpGMSed1	*G418*^{R} *GAP*$_{P}$–*MFα*(L42S)$_{SP}$–*T. reesei EGII–SED1*$_{A}$ *-AOX1*$_{T}$	This study
pIEG-PpGMG5	*G418*^{R} *GAP*$_{P}$–*MFα*(L42S)$_{SP}$–*T. reesei EGII–GCW5*$_{A}$ *-AOX1*$_{T}$	This study
pIEG-PpGMG12	*G418*^{R} *GAP*$_{P}$–*MFα*(L42S)$_{SP}$–*T. reesei EGII–GCW12*$_{A}$ *-AOX1*$_{T}$	This study
pIEG-PpGMG14	*G418*^{R} *GAP*$_{P}$–*MFα*(L42S)$_{SP}$–*T. reesei EGII–GCW14*$_{A}$ *-AOX1*$_{T}$	This study
pIEG-PpGMG19	*G418*^{R} *GAP*$_{P}$–*MFα*(L42S)$_{SP}$–*T. reesei EGII–GCW19*$_{A}$ *-AOX1*$_{T}$	This study
pIEG-PpGMG21	*G418*^{R} *GAP*$_{P}$–*MFα*(L42S)$_{SP}$–*T. reesei EGII–GCW21*$_{A}$ *-AOX1*$_{T}$	This study
pIEG-PpGMG28	*G418*^{R} *GAP*$_{P}$–*MFα*(L42S)$_{SP}$–*T. reesei EGII–GCW28*$_{A}$ *-AOX1*$_{T}$	This study
pIEG-PpGMG30	*G418*^{R} *GAP*$_{P}$–*MFα*(L42S)$_{SP}$–*T. reesei EGII–GCW30*$_{A}$ *-AOX1*$_{T}$	This study
pIEG-PpGMG34	*G418*^{R} *GAP*$_{P}$–*MFα*(L42S)$_{SP}$–*T. reesei EGII–GCW34*$_{A}$ *-AOX1*$_{T}$	This study
pIEG-PpGMG42	*G418*^{R} *GAP*$_{P}$–*MFα*(L42S)$_{SP}$–*T. reesei EGII–GCW42*$_{A}$ *-AOX1*$_{T}$	This study
pIEG-PpGMG45	*G418*^{R} *GAP*$_{P}$–*MFα*(L42S)$_{SP}$–*T. reesei EGII–GCW45*$_{A}$ *-AOX1*$_{T}$	This study
pIEG-PpGMG49	*G418*^{R} *GAP*$_{P}$–*MFα*(L42S)$_{SP}$–*T. reesei EGII–GCW49*$_{A}$ *-AOX1*$_{T}$	This study
pIEG-PpGMG51	*G418*^{R} *GAP*$_{P}$–*MFα*(L42S)$_{SP}$–*T. reesei EGII–GCW51*$_{A}$ *-AOX1*$_{T}$	This study
pIEG-PpGMG61	*G418*^{R} *GAP*$_{P}$–*MFα*(L42S)$_{SP}$–*T. reesei EGII–GCW61*$_{A}$ *-AOX1*$_{T}$	This study
pIEG-PpSSG34	*G418*^{R} *SPI1*$_{P}$–*SPI1*$_{SP}$–*T. reesei EGII–GCW34*$_{A}$ *-AOX1*$_{T}$	This study
pIH-EG-PpSSG34	*Hyg*^{R} *SPI1*$_{P}$–*SPI1*$_{SP}$–*T. reesei EGII–GCW34*$_{A}$ *-AOX1*$_{T}$	This study
pIU5-CBH1$_{D}$	*URA3 SED1*$_{P}$–*GLUA*$_{SP}$–*T. emersonii CBH1–SED1*$_{A}$–*SAG1*$_{T}$	(Liu et al. 2016)
pICBH1-PpSSG34	*G418*^{R} *SPI1*$_{P}$–*SPI1*$_{SP}$–*T. emersonii CBH1–GCW34*$_{A}$ *-AOX1*$_{T}$	This study
pIZ-CBH1-PpSSG34	*Zeo*^{R} *SPI1*$_{P}$–*SPI1*$_{SP}$–*T. emersonii CBH1–GCW34*$_{A}$ *-AOX1*$_{T}$,	This study

506 *A. aculeatus*, *Aspergillus aculeatus*; *T. reesei*, *Trichoderma reesei*; *T. emersonii*, *Talaromyces*

507 *emersonii*; P, promoter; SP, secretion signal peptide sequence; A, anchoring region; T, terminator,

508 *PrUbiC*, *Providencia rustigianii* chorismate pyruvate-lyase; *scFv*, single-chain variable fragment;

509 *GLUA*, *Rhizopus oryzae* glucoamylase; *MFα*, *S. cerevisiae* alpha-factor; *MjDOD*, *Mirabilis jalapa*

510 DOPA deoxygenase; *EcNMCH*, *Eschscholzia californica N*-methylcoclaurine hydroxylase

511

512

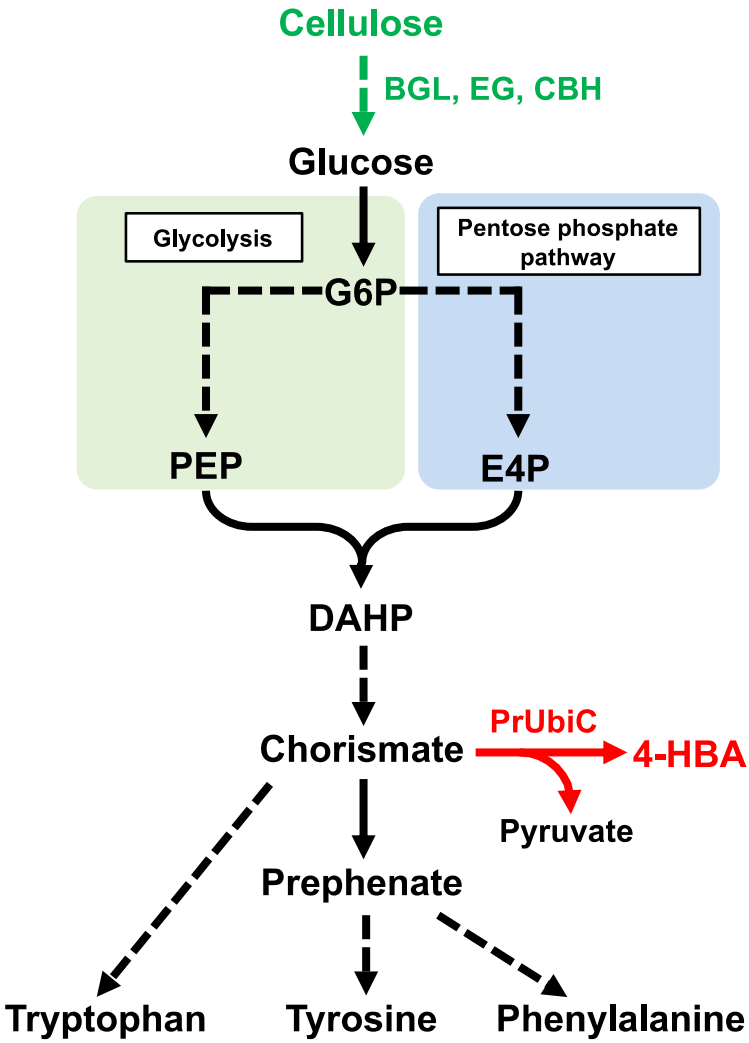

513

514 **Figure 1** Schematic pathway of 4-HBA biosynthesis in *P. pastoris*. Green and red arrows represent
515 reactions by heterologous enzymes. The dashed arrows indicate multiple enzymatic steps. G6P,
516 glucose-6-phosphate; PEP, phosphoenolpyruvate; E4P, erythrose-4-phosphate; DAHP, 3-deoxy-D-
517 arabinoheptulosonate 7-phosphate.

518

519

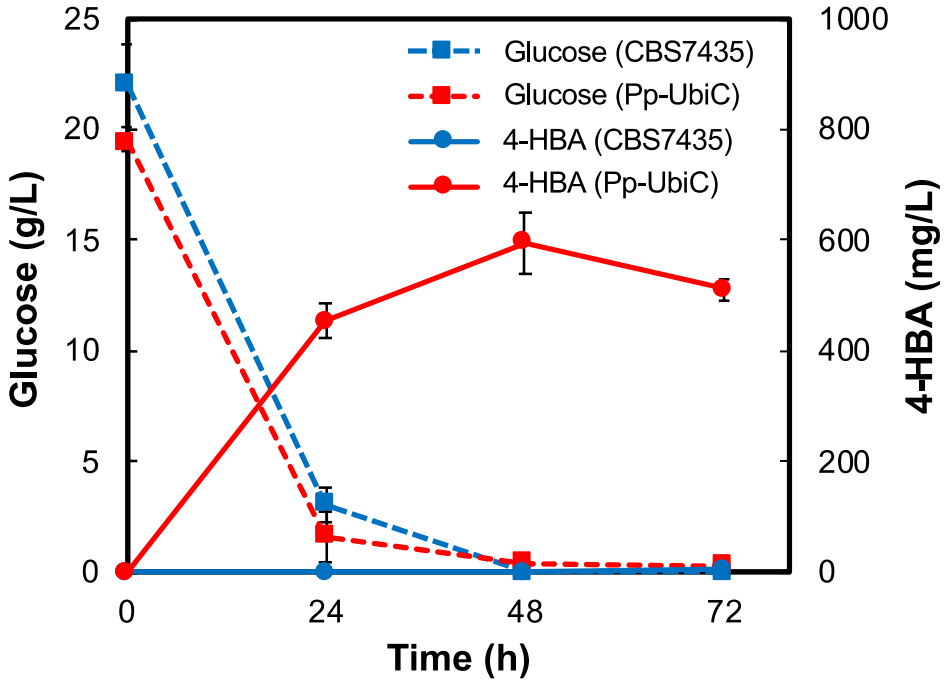

520

521 **Figure 2** Time course of 4-HBA production in YPD medium by *P. pastoris* strains.

522

523

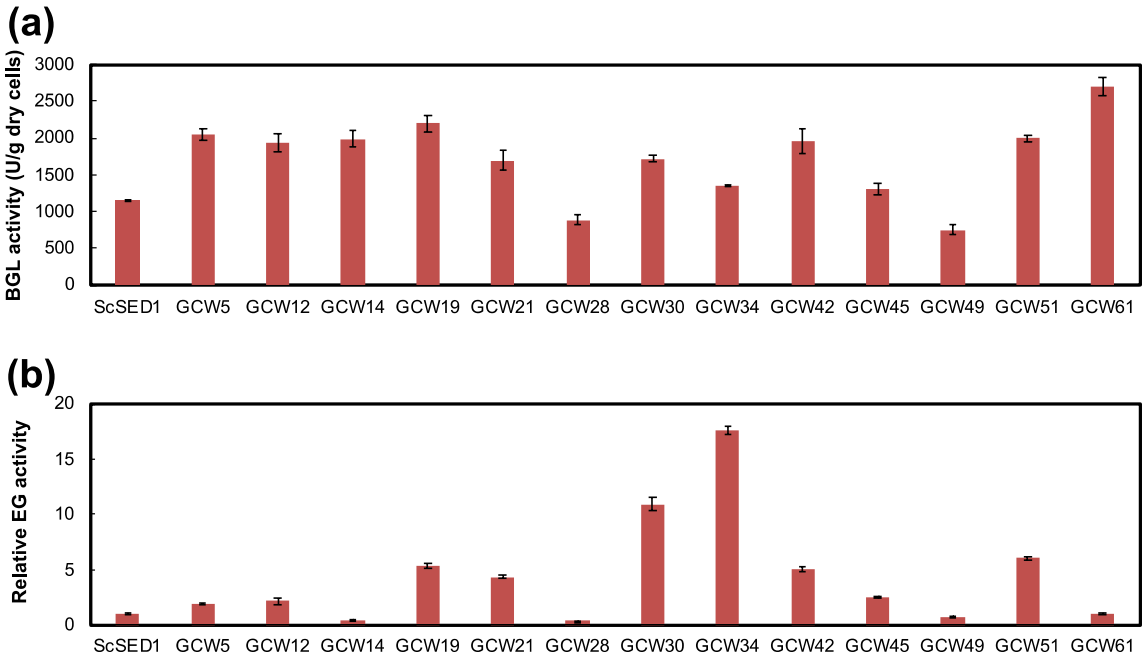

Figure 3 Comparison of cell-surface activity of **(a)** BGL and **(b)** EG. The enzymes were displayed using different GPI-anchoring domains in *P. pastoris* after cultivation in YPD medium for 48 h. The relative EG activity of each strain is shown as a fold-change in EG activity relative to the average level observed with strain Pp-EG-GMSed1 which uses Sed1p.

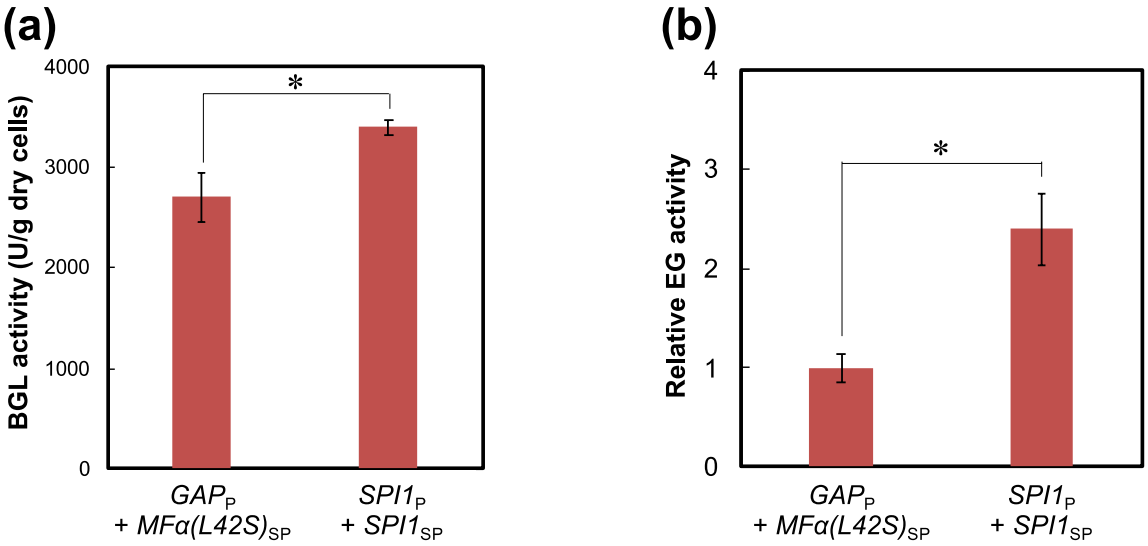

532

533

534 **Figure 4** The effect of replacing the promoter- and secretion signal sequences on cell-surface activity

535 of **(a)** BGL and **(b)** EG. *$p < 0.05$ for significant differences between two compared groups.

536

537

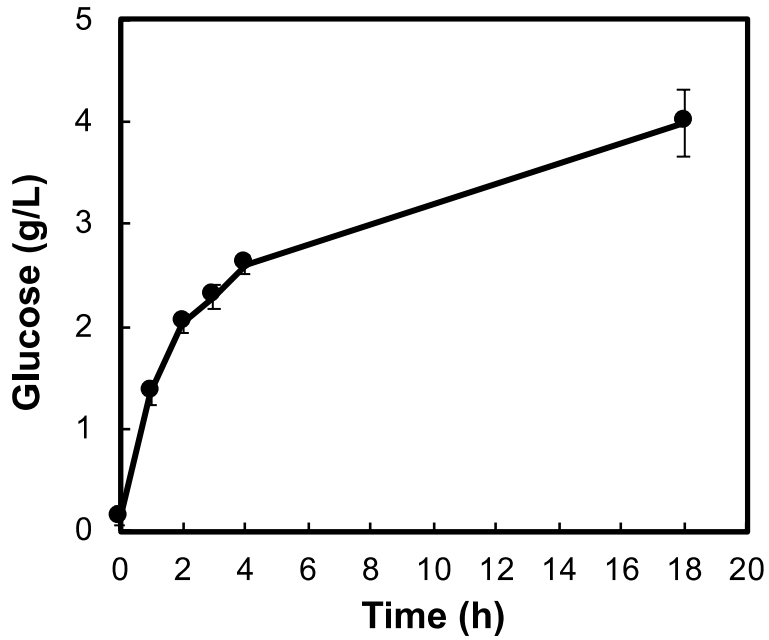

538

539 **Figure 5** PASCase activity of the BGL-, EG-, and CBH co-displaying *P. pastoris* strain (Pp-BEC).

540

541

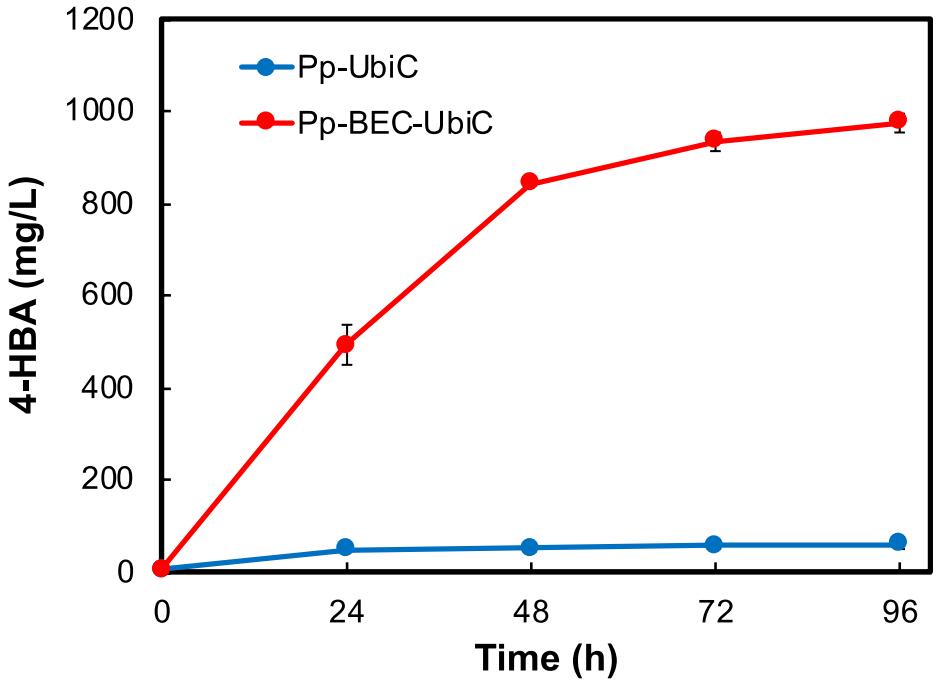

542

543 **Figure 6** Time course of direct 4-HBA production through SSF of 10 g/L PASC by Pp-UbiC and

544 Pp-BEC-UbiC strains.

545

546